Materials Research, Vol. 6, No. 1, 25-37, 2002.

New driving Parameters for Diamond Deposition Reactors: Pulsed Mode *versus* Continuous Mode

***Alix Gicquel*[a]*, *Khaled Hassouni*[a], *Guillaume Lombardi*[a],**

***Xavier Duten*[a], *Antoine Rousseau*[b]**

[a]*Laboratoire d'Ingénierie des Matériaux et des Hautes Pressions, UPR 1311, CNRS*
Université Paris 13 99 Avenue Jean Baptiste Clément 93430 Villetaneuse, France
[b]*Laboratoire de Physique des Gaz et des Plasmas,*
UMR 8578, Université Paris Sud, Bât 210, F91405 Orsay Cedex

Received: January 02, 2002; Revised: September 30, 2002

Experimental investigation and modeling of pulsed H_2/CH_4 plasmas used for diamond deposition are presented. Two plasma configurations are studied : a 2.45 GHz microwave cavity configuration and a 915 MHz surface-wave configuration. Time-resolved measurements of the gas temperature determined from the Doppler broadening of the Balmer -H_α line, of the H-atom relative density and of the discharge volume (V_{pl}) are reported. The experimental time-variations of the gas temperature are characterized by a sharp increase at the beginning of the pulse ($t < 250$ µs) and a decrease down to a stable value at steady state ($t > 1$ ms). The simulations enable us to estimate time-variations of the electron energy distribution function, gas temperature and chemical species densities. The in-pulse steady state temperature obtained from the model is in agreement with the measured one, although a discrepancy is obtained on the shape of the early time-variation. Calculations were carried out in order to study the effects of the in-pulse power, the duty cycle and the off-plasma time on the H-atom and CH_3-radical densities. It is seen that, at a constant power density averaged over a period, low duty cycles favor high H-atom and CH_3 - radical densities, while too long off-plasma times reduce the H-atom density during the pulse. In addition, the production of H atoms was seen to be governed by thermal dissociation in the 2.45 GHz microwave cavity system, and by electronic impact dissociation in the 915 MHz surface wave system, the latter operating under high gas velocities.

keywords: *diamond deposition process, microwave plasma, continuous mode versus pulsed mode, key parameters*

1. Introduction

The interest in CVD diamond films worldwide is undoubtedly due to the possibility of synthesis of a large variety of them. However, due to the relatively high cost of production in particular for very high quality and thick films, electronic industry remains still noncommittal about the use of this material. A better understanding of plasma reactors would certainly allow reducing the production cost. We present here a review that covers almost a ten-year period work dedicated to understanding the moderate pressure plasmas used for diamond deposition. Starting from the over-world accepted fact that H atoms and CH_3 radicals play major role for diamond growth in hot filament devices as well as in microwave plasma devices working at 1000 to 20000 Pa[1-4], our objective is to improve the densities of these species.

In continuous plasmas (cw), due to the high temperatures (2500 K to 3500 K) reached for power density greater than 15 Wcm^{-3}, H-atom production is mainly driven by thermal processes rather than by electronic processes[5]. However, due to the high gas temperatures reached in the plasma bulk, a significant increase of the reactor wall temperature is generally observed[6]. This strongly enhances the surface

*e-mail: gicquel@limhp.univ-paris13.fr

recombination processes and limits the excepted increase of the H-atom density due to the increase in dissociation yield. This drawback may be overcome by the use of pulsed discharges with a relatively low duty cycle (lower than 50%). Such discharges would enable to optimize the thermal heating so as to insure high enough H-atom production in the discharge with the lowest possible surface losses at the reactor walls[6]. The CH_3 radicals production is maximal for gas temperature ranging between 1800 K to 2000 K, and depends linearly on H-atom density[7]. These conditions are achieved at the plasma/surface interface.

The present paper is dedicated to the analysis of the changes occurring in the discharge characteristics and in the H-atom and CH_3-radical production efficiency when pulsed regime is used. After the experimental and modeling methods are provided, the paper is developed around three subsections. The first presents the approach and the results obtained in a continuous microwave plasma sustained in a cavity. Two types of modeling are presented in order to understand how the microwave power is coupled to the plasma, on the one hand and what are the kinetics of production and losses of the main species in the reactor on the other hand. In the second subsection is treated the effect of pulsing the plasma while the same configuration of microwave cavity is used. A time-dependant model is introduced, and the results are compared to the ones obtained for continuous mode. In particular, the effects of the in-pulse microwave plasma power and of the time-averaged power are studied. Finally, in the last section, using the same time-dependant model, another configuration for a pulsed plasma is studied. The excitation frequency is lowered from 2.45 GHz to 915 MHz, higher maximum in-pulse power is used (30 kW instead of 6 kW), and a surface-wave configuration is used instead of a cavity, in addition high gas velocities are used (up to 60 ms^{-1} instead of 1 ms^{-1}). In this section is studied the effect of the destruction of the H atoms during the off-plasma time, on the H-atom density during the on-plasma time.

2. Experimental setups – measurements

2.1- Experimental setups

The first plasma configuration (Fig. 1) consists of a quartz bell-jar surrounded by a cavity in which the microwaves (2.45 GHz) generated by a Sairem GMP 60 KE power supply are injected, with a maximum power of 6 kW[7]. The pressure ranges between 2500 and 20000 Pa, and for a given pressure value, the input microwave power is chosen in such a way to yield a constant ratio of the input power to the species density and a constant volume of the discharge (spherical shape in absence of the substrate holder of around 65 cm^{-3}). In pulsed mode, the duty cycle and the in-pulse power are monitored by a low-frequency voltage supply and followed by an oscilloscope. The couple power/pressure is varied from 2500 Pa/600 W to 20000 Pa/6 kW, and the gas flow and the maximum methane percentage are set to 200 sccm and 5%, respectively. The substrate temperature T_s is measured with a bichromatic pyrometer (IRCON), and its value is monitored by heating or water cooling the substrate.

The second device is depicted in Fig. 2[8]. The discharge is generated by a 915 MHz SAIREM power supply (GLP 300 KI) with a maximum output of 30 kW. The power is coupled to the plasma using a wave guide with a 6 cm diameter aperture, perpendicular to the wave propagation direction, where a tubular quartz reactor is introduced. Efficient power coupling and homogeneous plasma flow was

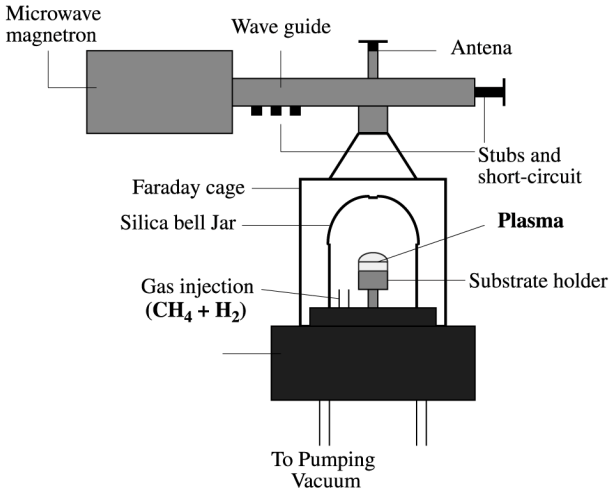

Figure 1. Microwave diamond deposition reactor in the cavity configuration. Excitation frequency of 2.45 GHz.

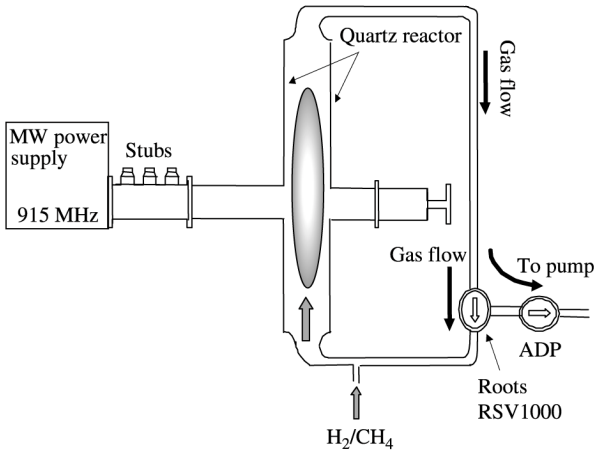

Figure 2. Reactor operating in a surface wave coupling configuration. Excitation frequency of 915 MHz.

obtained with a tube diameter of 5 cm diameter for a wide range of working pressure, i.e. p = 5000-10000 Pa, and a power varying between 5 and 30 kW. These input power values may result in high plasma temperature and an overheating of the reactor wall. Therefore, a double envelope quartz tube cooled with a low microwave absorption silicon oil was used. The feed gas is pumped in a constant-pressure closed circuit using a high pumping speed primary root. High gas flow velocity (5-60 ms^{-1}) is used that yields further heat dissipation through the heat convection flux transported by the gas exhausting the reactor. The residence time in the discharge ranges between 0.1 and 0.5 s for the experimental conditions routinely adopted in this system.

The plasma may be operated either in a continuous wave (cw) or a pulsed wave (pw) regimes. The pulse period and duty cycle may be varied in the ranges 3-30 ms and 1-100%, respectively. When operating in pw regime at 30 kW, a residual input power of 3 kW is maintained during the out-pulse time. This is necessary for providing a quasi-square pulse with a fast ignition time at high in pulse power. Note that the ignition time is always less than 25 μs, which is the time required by the power supply to increase the input-power from 3 kW to the in-pulse power value. In this work we will mainly focus on the study of the pulsed mode.

2.2- Measurement-Experimental Validation

The H_2-CH_4 plasmas obtained in the device described above were investigated experimentally by optical emission and absorption spectroscopy. For this purpose, a THR 1000 Jobin Yvon monochromator equipped with a 1800 gr/mm grating along with a Hamamatsu R928 photo-multiplier were used to detect the plasma emission signal. Time-resolved emission spectroscopy was used to track the temporal evolution of the emission intensities of H_α line (IH_α), $H_2(G^1\Sigma_g^+\text{-}B^1\Sigma_u^+)$ band, $C_2(d^3\Pi_g\text{-}a^3\Pi_u)$ Swan band and $CH(A^2\Delta - X^2\Pi)$ band. Argon was introduced at very low amount in the discharge and its 750 nm emission line was used as an electrical calibrator for performing actinometry measurements and reach H atom relative densities, once this method has been validated by TALIF[9].

For the 915 MHz device, the gas temperature was determined from the rotational structure of the absorption band of the $C_2(a^3\Pi_u)$ low-energy state (0.09 eV above ground state). Under the considered discharge conditions, i. e. p > 500 -10000 Pa, the rotational mode of this low-energy state and the translation mode of heavy species may be assumed in thermal equilibrium. Absorption techniques enable therefore a direct determination of the gas temperature along with $C_2(a^3\Pi_u)$ density[10].

The absorption experiments were performed using an OSRAM stabilized xenon arc lamp as a light source. They additionally required the use of a EG&G CCD detector instead of the photo-multiplier for enabling data accumulation and signal enhancement. The determination of gas temperature using absorption measurement requires integration time typically above 2 ms. Consequently absorption was only used for cw discharges. The comparison between the gas temperature determined with this technique and the rotational temperatures of several excited states of carbon containing species (C_2, CH and CN-nitrogen being added as an impurity) and H_2 molecule (especially the $d^3\Pi_u$ state of the Fülcher-α system and the $G^1\Sigma_g^+$ state) showed that the rotational temperature of the $G^1\Sigma_g^+$ state of the H_2 molecule could be used as an indicator of the gas temperature for the conditions used[11]. Consequently, the rotational temperature of the $G^1\Sigma_g^+$ state was used in pw mode.

In the 2.45 GHz device, the gas temperature was determined by the Doppler broadening of the H_α emission line (656.3 nm ; H(n = 3)=>H(n = 2)), after this method has been validated by Talif[9]. For the pw mode, we assumed that the thermal equilibrium between H(n = 1) and H(n = 3) still takes place for pulsed mode discharge[6]. This assumption would be valid at least for high enough delay after the discharge ignition when the time-variation are smooth enough and H(n = 3) excitation proceeds through electron-impact collision with H(n = 1). The thermal equilibrium assumption could be however questionable for a very short delay, immediately after the discharge ignition, where "hot" H-atom may be created through dissociative excitation of either H_2 or CH_4. This assumption is discussed in Ref. 6. In addition, CH_3 radical densities have been measured by UV absorption spectroscopy, but only in cw mode[6,12-14].

In pw mode, the time-variation of the discharge volume was measured using a set of pictures taken at frequency of approximately 30 kHz using a "Flashcam" (from PCO Computer Optics) (Fig. 3). The time-variation of both volume and MWPD are reported in Fig. 4[6]. The volume-values determined from the discharge pictures are used for the estimation of the variations of the average power density. They have been calibrated by the power density value previously determined for a continuous-mode discharge obtained at 800 W and 3200 Pa, which is the same as that obtained for the steady state in-pulse discharge.

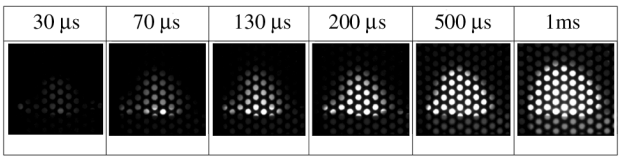

Figure 3. Ignition of the plasma ball, observed thanks to a "Flashcam". Plasma conditions: in-pulse power 800 W, 3200 Pa, MicroWave Power Density (MWPD) = 12 Wcm^{-3}.

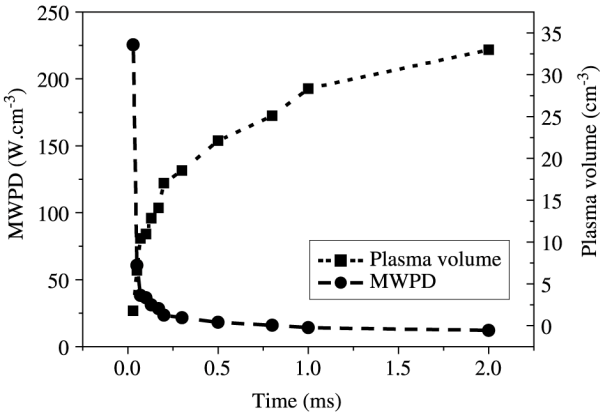

Figure 4. Evolution of plasma volume and MWPD as a function of the time. Plasma conditions: in-pulse power 800 W, 3200 Pa, power density of 12 Wcm^{-3}.

3. Plasma Modeling

3.1 Plasma Modeling in continuous mode and for a cavity configuration

In order to understand the different phenomena which occur in microwave cavity plasmas typical for diamond deposition operating in cw mode, two models have been developed: a 2D self-consistent diffusive H_2 plasma model[15] and a non-self-consistent one-dimensional diffusive/convective $CH_4 + H_2$ plasma model[5].

The first model enabled us to understand how the energy is deposited into the plasma and to determine the main processes which control electron energy and density, gas heating, hydrogen dissociation and plasma/surface energy transfers. The second model, which involved input data provided by the self-consistent model or by experimental measurements, enabled us to understand the chemical kinetics and transport of H-atoms and carbon-containing species. The physical model used in the latter model describes the thermal non-equilibrium of this kind of plasma by taking into account three energy modes: the translation-rotation mode of heavy species ('t-r'), the vibration mode of molecules ('v') and the translation mode of electrons ('e'). The 't-r' and 'v' modes are described by a Maxwell-Boltzmann distribution function with two different temperatures, respectively denoted T_g and T_v. For the 'e' (electronic) mode, the electron energy distribution function (EEDF) is determined for several discharge conditions by solving the electron Boltzmann equation for the $H_2/H/CH_4$ system[16,17]. The electron-heavy species collision rate constants are then curve-fitted as a function of the electron average energy. The use of these curve-fit along with a balance equation for the electron average energy enables us to take into account the non-Maxwellian behavior of the EEDF.

As far as chemistry is concerned, the kinetics model used in this work is similar to that of Ref. 5. The chemical non-equilibrium of the plasma is described by taking into account 31 chemical species and 134 reactions. The chemical model involves three groups of reactions. The first corresponds to the chemical model necessary to describe a pure hydrogen plasma, while the second group describes the thermal cracking of methane and takes into account $CH_{y=0\,4}$ and $C_2H_{y=0\text{-}6}$ neutral species. The third reaction group consists of collisions involving charged species such as electron impact ionization and dissociation of hydrocarbon species, ion conversion processes and dissociative recombination of hydrocarbon ions[16,17].

3.2- Plasma Modeling in pulsed mode

The physical plasma model used for H_2-CH_4 pulsed plasma extends that previously mentioned. In principle, the prediction of the time-variation of the plasma characteristics requires the solution of the time-dependant transport equations for the chemical species, the flow momentum components and the total energy. In addition, the electron Boltzmann equation and an electromagnetic model that enable to describe the plasma-wave interaction and the electron heating should be considered and coupled to the plasma transport equations. This leads, for a two-dimensional geometry, to a quite complex and intractable numerical problem that is out of the scope of this work. We focused on the investigation of the plasma dynamic in a pulsed wave regime, that is on the determination of the time-variation of species densities, gas temperature and eedf in the bulk of the plasma. For doing so, a Nusselt model was used to describe the plasma flow in the case of the 915 MHz surface wave configuration device[8].

The Nusselt model used to describe the plasma flow in a cylindrical reactor assumes a radial homogeneous plasma volume and a linear boundary layer where all the plasma parameters are assumed to vary linearly. The thickness of the boundary layers is in addition assumed to remain constant along the reactor (Fig. 5). Under these assumptions, the concentration of a given species only depends on the residence time, t, in the reactor. This latter is related to the axial position through the relation $t = z/\langle v \rangle$, where $\langle v \rangle$ is the radially averaged plasma flow velocity. The time-variation of species population in the bulk of the plasma is equal to the total net production rates due to gas phase chemistry and to catalytic reactions on the reactor wall. This may be expressed using the following ordinary differential equation :

$$\frac{dY_s}{dt} = \frac{W_s - R_s}{\rho} \qquad (1)$$

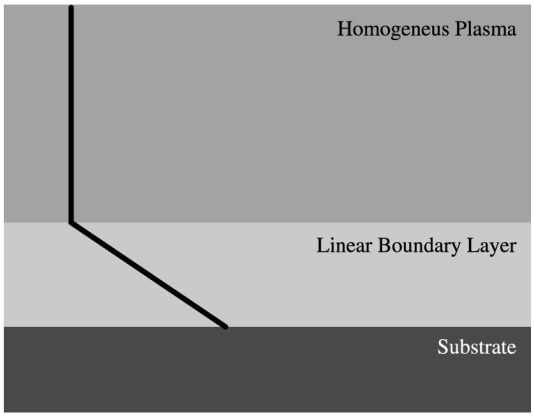

Figure 5. Principle of the Nusselt model

where Y_s and W_s denote the mass fraction and the mass production rate by gas phase reaction in the bulk of the plasma for species 's', respectively. *r* is the plasma total mass density. R_s is the mass production rate of species 's' by surface reactions at the reactor wall. Its determination requires the estimation of the rates, r_r, for all the surface reactions, 'r', of the model.

In this work we have considered catalytic recombination reactions for atoms, charged species and unstable radicals. The surface reactions are especially important in the case of H-atom and charged species, the consumption of which is mainly due to recombination on the reactor wall. The rate of a surface recombination reaction 'r' of a species 's' may be expressed as:

$$r_r = D_s \frac{c_s - c_{s-w}}{\delta} \frac{2}{R-\delta} M_s \qquad (2)$$

where D_s, c_s, c_{s-w} and M_s are the diffusion coefficient, the bulk concentration, the surface concentration and the molar mass of the recombining species 's'. R is the reactor radius and δ is the diffusion boundary layer thickness.

The estimation of r_r requires the determination of species 's' concentration at the reactor wall. This latter may be related to the bulk concentration through the following relation which expresses the equality between the rates of diffusion flux and recombination at the reactor wall:

$$D_s \frac{c_s - c_{s-w}}{\delta} = \frac{\gamma_r}{4} \sqrt{\frac{8RT_w}{\pi M_s}} c_{s-w} \qquad (3)$$

Where γ_r is the recombination coefficient for reaction 'r', T_w is the wall temperature and R the gas constant.

The ions recombine totally on the reactor wall and their recombination coefficients were then taken equal to 1. The recombination coefficient of H-atom on quartz was taken from Ref. 18 ($\gamma_H = 10^{-4}$). There is practically no data on the recombination coefficients of hydrocarbon radicals on quartz surface. We therefore assumed a value of 10^{-3} similar to that found for CH_3 recombination on diamond for the recombination probability of all the hydrocarbon radicals. This assumption should not have an important consequence on the model results since, as reported in Ref. 18**,** surface reactions have almost no effect on the kinetics of hydrocarbon species under moderate pressure discharge conditions.

The diffusion boundary layer thickness for hydrogen species (H_2, H, H^+, H_2^+ and H_3^+) were estimated using the one-dimensional model of reference[5,8,9]. This model yields, in the case of the investigated device (R = 5 cm), a diffusion boundary layer thickness of 2 cm for H-atom and of 5 mm for H^+ and H_3^+ ions. As far as hydrocarbon species are concerned, we assumed a boundary layer thickness of 2 cm for neutral species and 5 mm for ions. This assumption should also not affect the results since the populations of these species are mainly governed by gas phase reactions.

The diffusion coefficients were determined by using the collision integrals given by Yos for hydrogen species[19], while Lennard-Jones potential was assumed for estimating the diffusion coefficients of hydrocarbon species. Due to the relatively high pressure of the considered discharges, ambipolar diffusion was assumed for charged species, the diffusion coefficients of which were corrected by the factor $(1+2/3<\varepsilon_e>/kT_g)$ where $<\varepsilon_e>$ is the average electron energy, T_g the gas temperature and k the Boltzmann constant.

The estimation of W_s in equation (1) requires the determination of the rate constants, k_j, of all the reactions involved in the chemical model described in the previous section. These rate constants may depend either on the eedf in the case of the processes involving electrons or on the gas temperature for the processes involving only heavy species. In the present model, the eedf is determined from the solution of the time-dependant electron Boltzmann equation[16,17].

Finally, the total energy equation that governs the time-evolution of the gas temperature in the frame of the model used in this work is written as:

$$\sum_{i=1,n_s-1} \rho Y_i Cp_i \frac{dT_g}{dt} + \sum_{i=1,n_s-1} \rho \, x \frac{dY_i}{dt} h_i + \rho Y_e Cp_e \frac{2}{3k} \frac{d<\varepsilon_e>}{dt} + \rho Cp_e \frac{2}{3k} <\varepsilon_e> \frac{dY_e}{dt} =$$
$$PMW - \lambda \frac{(T_g - T_w)}{\delta_t} \frac{2}{R} - \sum_{i=1,nrs} v_i \Delta H_i \frac{2}{R} \qquad (4)$$

The left hand side (LHS) of equation (4) represents the time-variation of the total energy that includes four compo-

nents: two components corresponding to the change of heavy species temperature and electron average energy and two other terms corresponding to the heavy species and electron participation to the total change of the plasma enthalpy due to chemical reactions. The right hand side (RHS) of equation (4) includes the electomagnetic power absorbed by the plasma (PMW) and two terms that represent the energy loss by conduction and enthalpic species recombination at the reactor wall. The data references necessary to solve the problem can be found in Ref. 18.

In the expression of the different terms described above, Cp_i and h_i denote the specific heat and the formation enthalpy of a heavy species 'i' respectively. ΔH_i and v_i denote the rate and reaction-enthalpy of surface reactions, respectively. Cp_e and $<\varepsilon_e>$ are the electron specific heat and average energy and k is the Boltzmann constant. The heat loss due to conduction to the reactor wall depends on the thermal conductivity and the thermal boundary layer thickness. The thermal conductivity was also estimated by using the collision integrals proposed by Yos for hydrogen species[19] and Lennard-Jones interaction potential for hydrocarbon species. The thermal boundary layer thickness was also estimated from the one-dimensional model of reference[20]. A value of 2 cm, similar to that of the boundary layer thickness of H-atom, was found for δ_t.

3.3 Bell jar configuration versus *tubular reactor*

The thermochemical non-stationary quasi-homogeneous plasma models used in this work are rather similar for both the 915 MHz and 2.45 GHz frequency devices. The main difference consists in the adaptation made to take into account for the geometry of the reactors: a tubular reactor and, a bell jar respectively[6].

For the bell jar reactor, the ratio of the plasma volume to the substrate surface necessary to estimate the rates of surface chemical processes was determined by considering that the discharge is a spherical cap located just above the substrate surface, and the time-variation of the power density in particular at the beginning of the pulse (estimated experimentally) was taken into account. In the tubular reactor operating with a surface wave configuration at 915 MHz, the ratio of the plasma volume to the substrate surface was easily calculated but the power density was considered to be constant during the pulse since it could not be estimated experimentally.

For a given set of experimental conditions (pressure, input power, time-variation of the plasma volume), numerical simulation solves, for the coupled set of non-stationary Boltzmann equation, species kinetics equations and a total energy equation. This enables the estimation of the time-variation of the eedf, the species density, the reduced electric field and the gas temperature[6].

4. Results

4.1 Continuous mode: cavity configuration, excitation frequency of 2.45 GHz

4.1.1 H-atom density and gas temperature

Axial variations in microwave power density, electron density and temperature as well as gas temperature and H-atom mole fractions extracted from the 2D self-consistent model are shown in Fig. 6a, 6b, 6c, 7a and 7b respectively for different power-pressure pairs[15,21]. The results show that, while microwave power is mainly deposited in the near surface region and the electron temperature follows this behavior rather well, the gas temperature is maximal in the plasma volume. The atomic hydrogen density is also maximal in the plasma volume and sharply decreases in the near surface region due to catalytic surface recombination reactions. The plasma electron density is around 10^{12} cm^{-3}, the major ion being H_3^+ in a large range of plasma conditions. The results also show that hydrogen dissociation strongly depends on the microwave power coupled to the plasma (Fig. 7b).

Although results obtained from the 2D self-consistent model are qualitatively in agreement with those obtained from the 1D model[5], some quantitative discrepancies can be observed. In particular, 1D model calculations provide higher values of H-atom mole fraction than the 2D self-consistent model calculation do (at 8400 Pa and 1500 W which corresponds to an average power density of 22 Wcm^{-3}, the 2-D model leads to 3% of H atoms and the 1D model to 8.5%). A comparison with experiments shows a better agreement with the results from the 1D model, in particular when the microwave power distribution function is deduced from experiments. We attribute the discrepancy to the sensitivity of the 2D self-consistent model to the geometric configuration of the cavity. As a matter of fact, very small error on the base plate or the antenna position may result in quite significant error in the spatial distribution of the power density and, therefore, on the estimate of the plasma temperature and composition. In particular, the 2D self-consistent model shows that the microwave power coupled in the emissive plasma volume is typically 80-90% of the total input power. The remaining 10-20% of the input power is absorbed outside this region and especially near the top wall of the quartz vessel. As a consequence, there might be a significant discrepancy between the power density distribution calculated with the 2D self consistent model and the power density distribution used in the 1D model. In any case the two models yields quite comparable results and almost the same qualitative conclusion on the evolution of the plasma behavior as function of the process parameters.

Finally, for the following, we will retain results from the 1D model which allowed us to simulate the plasma

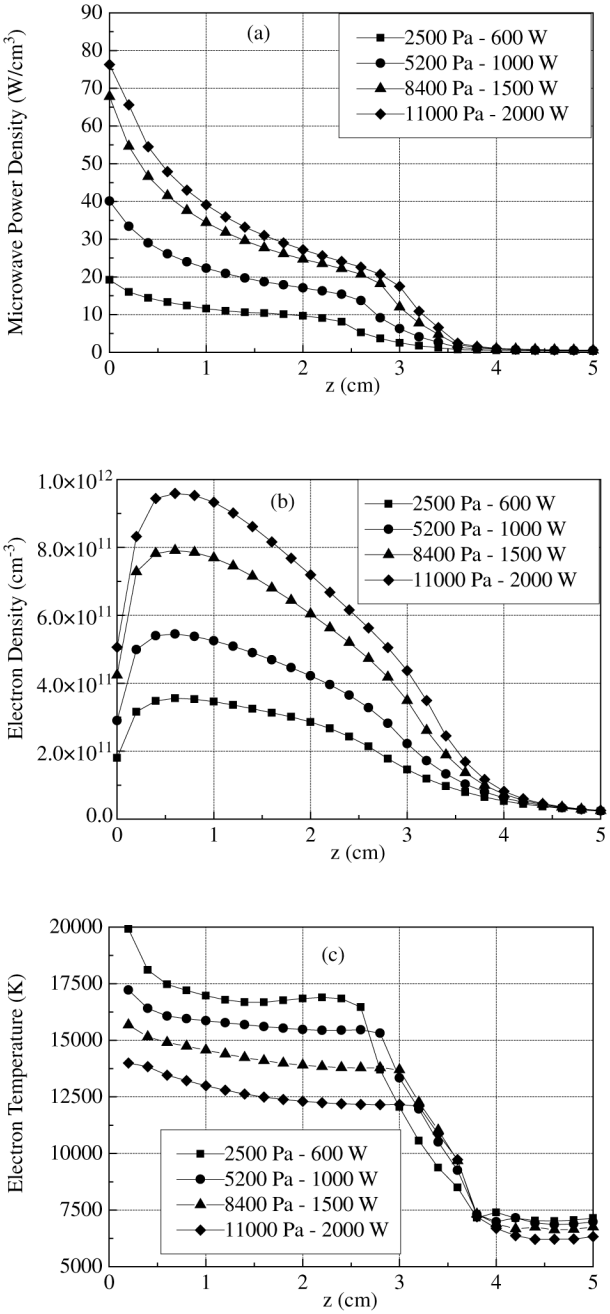

Figure 6. Simulated variations, on the reactor axis, of some discharge characteristics vs position above the substrate (z) for different power – pressure pairs (a) absorbed power density; (b) electron density; (c) electron temperature.

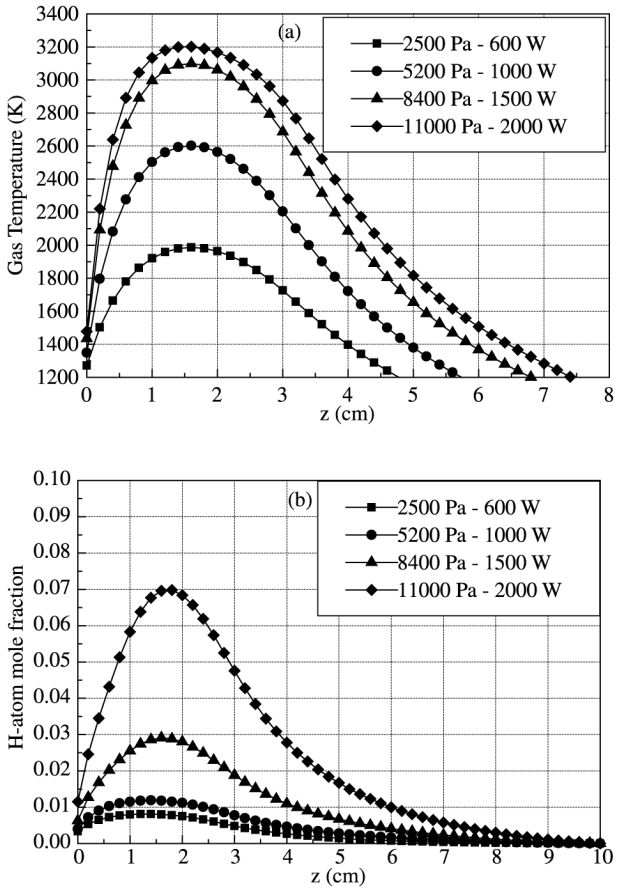

Figure 7. Simulated variations of (a) gas temperature; (b) H-atom mole fraction, on the reactor axis, *vs.* position above the substrate (z) for different power – pressure pairs.

behavior in H_2 + CH_4. The variations in the H-atom mole fraction with power density calculated from the 1D model are shown in Fig. 8a. The H-atom mole fraction in the plasma volume is seen to vary from 1 to 12% as the power density is increased from 9 to 30 Wcm^{-3} (Fig. 8a), and simultaneously the gas temperature in the plasma volume increases from 2200 K to 3400 K (Fig. 8b). These behaviors associated with the behavior of the electron temperature (Fig. 6c) indicate a change in the dissociation mechanism as the power density is increased. Indeed, the sharp increase in the production of atomic hydrogen must be related to the sharp increase in the gas temperature in particular, while the latter surpasses 2200 K, since, in contrast, the electron temperature decreases. Thus, our conclusions are that the dissociation of molecular hydrogen is governed by electronic processes, while the pressure and gas temperature remains below 2000 Pa and 2000 K respectively. In contrast, thermal dissociation is predominant, as power density leads to a gas temperature higher than 2500 K.

Due to the decrease in the gas temperature and to the surface atom recombination at the diamond surface, a decrease in H-atom mole fraction is observed in the near surface region (Fig. 7b). Finally, as a first approximation, we

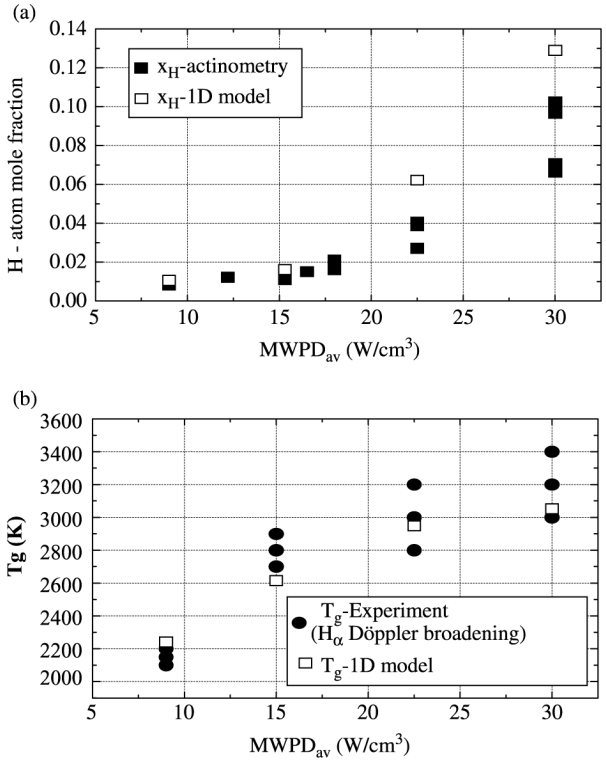

Figure 8. Variations of (a) H-atom mole fraction; (b) gas temperature vs averaged power density.

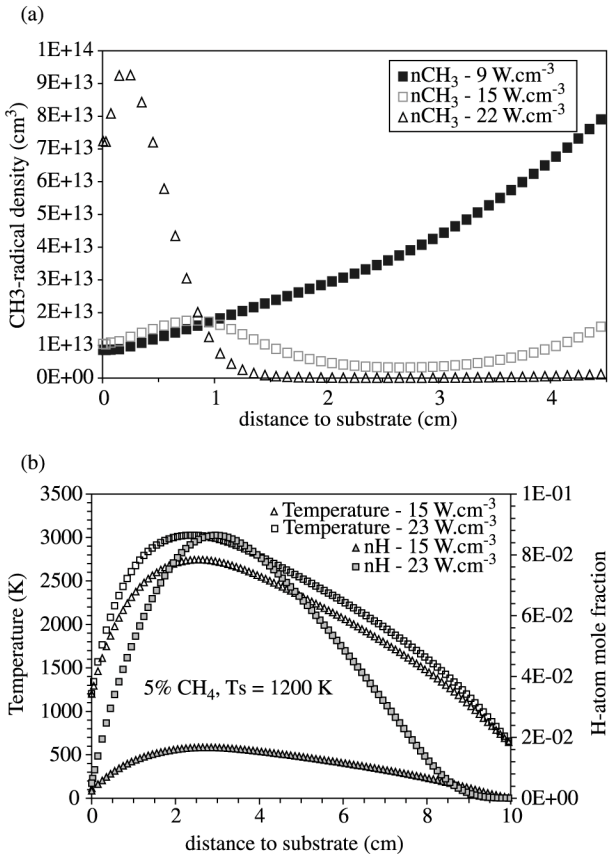

Figure 9. (a) Axial distributions of CH_3-radical density for three averaged power densities; (b) H-atom mole fraction and gas temperature axial distributions calculated from 1D H_2 + CH_4 plasma model, for three power densities.

can admit that H-atom density at the surface is mainly controlled by the processes of production in the plasma volume (that depend on either on the electron temperature or the gas temperature) and by diffusion in the near surface region. Note, however, that, in contrast to the hot filament reactor, in this kind of system, as high electron temperature exists in the near surface region (Fig. 6b), electronic dissociation processes may act as a brake for the disappearance of atomic hydrogen in this region.

4.1.1 Carbon containing species

For all the discharge conditions considered in this work, the major hydrocarbon species is C_2H_2; its value is approximately two times less than that of methane introduced in the feed gas and is practically constant in the discharge[4]. In contrast, the axial density profiles of the other hydrocarbon species show very strong variations, several orders of magnitude for some species. These variations are strongly linked to that of the gas temperature.

Figure 9a shows profiles of calculated CH_3-radical density along the reactor for three power densities (MWPD)[4]. As observed experimentally, for 15 Wcm^{-3} and 22 Wcm^{-3}, an increase in the methyl-radical density appears in the near substrate region (at around 2 mm/substrate). Experimental and calculated results lead support to the conjecture that methyl radical concentration is tightly coupled to the hydrogen dissociation fraction and to the gas temperature (Fig. 9b), in accordance with the partial equilibrium of the hydrogen abstraction reactions :

$$CH_4 + H \leftrightarrow CH_3 + H \quad (5)$$

$$CH_3 + H \leftrightarrow CH_2 + H_2 \quad (6)$$

$$CH_2 + H \leftrightarrow CH + H_2 \quad (7)$$

$$CH + H \leftrightarrow C + H_2 \quad (8)$$

Thus, the linear variation of CH_3-radical density as a function of methane percentage observed in reference[7] is attributed to the shift in reaction (5) towards the production of CH_3, since the H-atom density remains constant as a func-

tion of methane percentage. As well, the increase and the shift towards the surface in CH_3-radical density with power density observed in the near surface vicinity (Fig. 9a) is attributed to the steeper gradient in the gas temperature and the increase of the H-atom density as the power density increases (Fig. 9b) (shift in the reaction (5) towards the right). However, as the gas temperature becomes greater than 2000-2200 K, reaction (6) is also shifted to the right, resulting in a decrease in CH_3-radical density. Thus, the strong decrease in CH_3-radical density in the plasma volume (at 20 mm from the substrate) is attributed to the strong increase in the gas temperature with power density (from 2200 K to 3200 K as power density increases from 9 to 22 Wcm^{-3}) that promotes dissociation of CH_3.

From these results, we can draw some conclusions concerning the surface H-atom and CH_3-radical densities controlling parameters, in cw mode. While H-atom density at the surface is mainly governed by its production in the plasma volume (controlled by the gas temperature and/or the electron temperature) and by a diffusion process in the near surface region, methyl radical density is mainly governed by gas-phase thermally activated reactions occurring in the near-substrate region (although the gas temperature gradient itself is controlled by diffusion processes).

4.2 Pulsed mode: cavity configuration, excitation frequency of 2.45 GHz[6]

Up to now, only few sets of experimental conditions have been analyzed, and the results presented here correspond to a pressure of 3000 Pa, an input power of 800 W and a feed gas composition of H_2:CH_4 = 95:5. The diamond substrate temperature was set to 1000 K, which corresponds to a surface recombination coefficient of 0.1 for H-atom[18].

Figure 10 shows the calculated time-variation of the gas temperature for duty cycles varying from 17% to 70%. Comparison with the temperature measured from the Doppler broadening of H_α emission line with a duty cycle of 17% shows that although a very good agreement is obtained for the steady state in-pulse value, there is a substantial discrepancy on the value of the maximum temperature during the strong heating phase. As a matter of fact, while the H(n = 3) shows a maximum value of 3000 K corresponding to an overheating of 800 K with respect to steady state, the model only yields a maximum of 2300 K corresponding to an overheating of 100 K. Many explanations involving criticism of either the experimental method used to determine the temperature or some uncertainty in the experimental plasma volume, are discussed in Ref. 6.

Beyond the different explanations, the most probable is the following: once all the microwave power is transferred into the discharge (after 30 μs), the plasma ignites just above the substrate in a very small region with a strong electric

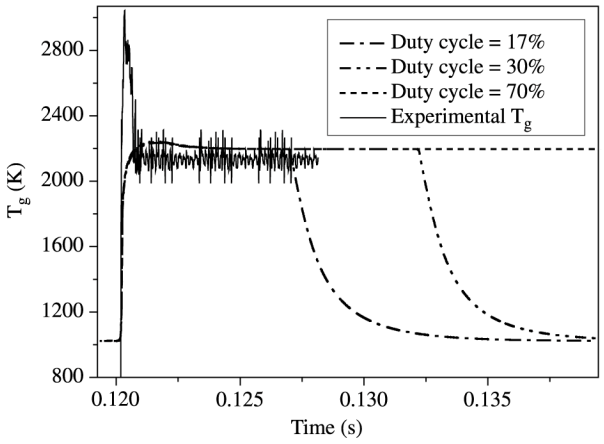

Figure 10. Comparison between calculated and experimental time-resolved H_α temperature (gas temperature). Experimental plasma conditions: in-pulse power 800 W, 3200 Pa, power density = 12 Wcm^{-3}; duty cycle 17%; 2 cm from substrate. Calculations performed for duty cycles of: 17%, 30% and 70%.

field (where the reduced field E/N is the highest[6]). Therefore, during the first stage, the 800 W microwave power are coupled in a small volume above the substrate (Fig. 4). This results in a considerably high local MWPD values and consequently in a strong gas heating and a high gas temperature. The second phase of the discharge is characterized by the increase of the plasma volume and a subsequent decrease of MWPD and gas temperature. In this case, the obtained discrepancy could be attributed to some uncertainty in the experimental estimation of the plasma volume. The time-variations obtained from simulations are indeed strongly sensitive to the input values of the volumetric power density which may be subject to a substantial error with an important consequence on the predicted T_g value, especially in the early stage of the pulse. Also, the assumption of quasi-homogeneous plasma may break down during this early stage where the plasma volume undergoes a quite strong expansion. If the quasi-homogeneous plasma assumption breaks down during the early stage of the pulse, the improvement of the description of this phase requires at least the use of 1D model that would properly describes the discharge expansion and the spatial non-homogeneity.

In any case the present model gives satisfactory prediction of the steady state in-pulse values. In addition, the steady state in-pulse values are identical to those obtained in cw plasma, and they depend only on the in-pulse power density and not on the power density averaged over a period as this has been demonstrated in Ref. 6. On the contrary, the wall temperatures depend on the time-averaged power den-

sity, and not on the in-pulse power density[6].

4.2.1 Influence of the duty cycle on gas temperature and active species densities

To study the effect of the in-pulse power on the production of H-atoms and CH_3 radicals, the time-averaged input microwave power was set constant to 600 W averaged over a constant period of 20 ms, while three values of duty cycle were tested: 30, 50 and 70%, with in-pulse durations of 6, 10 and 14 ms respectively. The corresponding in-pulse powers were then 2 kW, 1,2 kW and 850 W respectively.

Figure 11a shows the H-atom density obtained for several duty cycle values. The H-atom density strongly increases as the duty cycle is decreased, and reaches 1.8 $\times 10^{16}$ cm^{-3} for a duty cycle of 30%, and 10^{15} cm^{-3} for a duty cycle of 70%. It is attributed to the increase in the gas temperature with the in-pulse power, the temperature being maximal at low duty cycle as shown in Fig. 12. Indeed, under these conditions, the main H_2 dissociation mechanisms is thermal, and at a duty cycle of 30%, it is seen that T_g reaches 2800 K, while at a duty cycle of 70%, it reaches only 2250 K. Simultaneously, the corresponding H-atom mole fraction are 7% and 1% respectively. These properties of pulsed discharges may be interesting for the deposition of high quality diamond.

We can observe in Fig. 11b the same behavior for CH_3, with a density increased by a factor of 5 when the duty cycle varies from 50% to 30%, for the power density of 600 W, averaged over the period. The production of the methyl radical is indeed mainly governed both by the gas temperature (in the range 1800 K - 2000 K) and the H-atom mole-fraction, these ranges are reached, for the duty cycle of 30%, during the first 250 µs.

4.3 Pulsed mode: surface wave configuration, excitation frequency of 915 MHz

Calculated and measured gas temperatures were compared, as in the previous section, for discharge conditions corresponding to an average MWPD of around 12 Wcm^{-3}: duty cycle of 10 %, discharge duration of 3 ms, in-pulse power of 12 kW, off-pulse power 3 kW, pressure 2000 Pa (Fig. 13). Again, a good agreement is observed for the steady state temperature while a discrepancy appears during the strong heating of the gas (first 500 µs). The discrepancy is here still stronger than in the previous case since the calculations do not take into account the variations of the plasma volume at the ignition.

It is worth noting that, for almost the same MWPD as for the cavity configuration, the steady state gas temperature reached during the pulse is almost identical (2200 K), confirming that the gas temperature is controlled by the in-pulse power density.

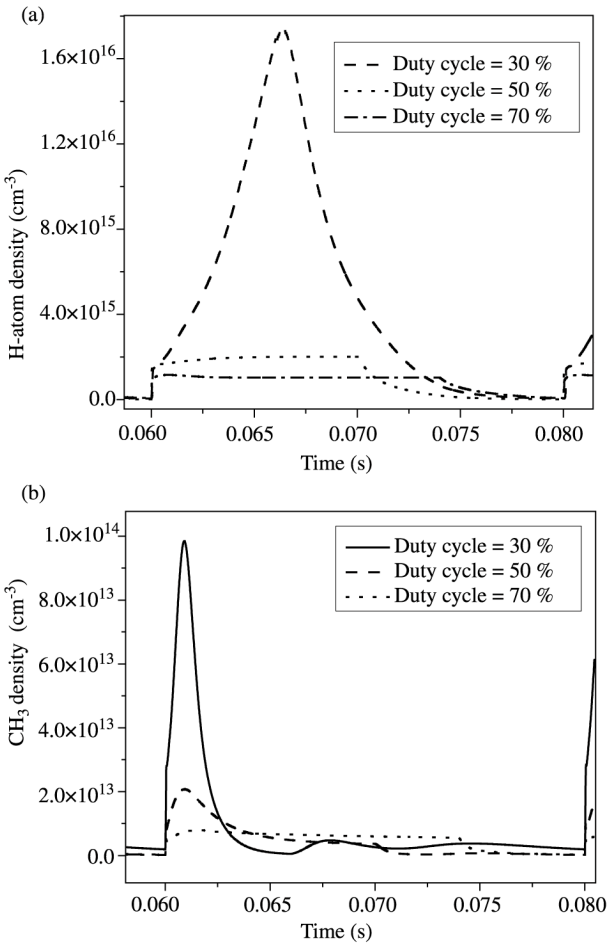

Figure 11. (a) Calculated H-atom density for different duty cycles; (b) calculated CH_3-radical density for different duty cycles, at a constant average microwave power of 600 W.

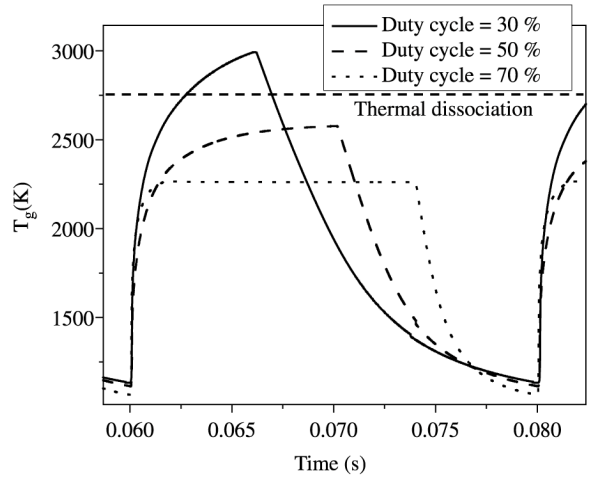

Figure 12. Evolution of the gas temperature as a function of the duty cycle, at a constant average microwave power of 600 W.

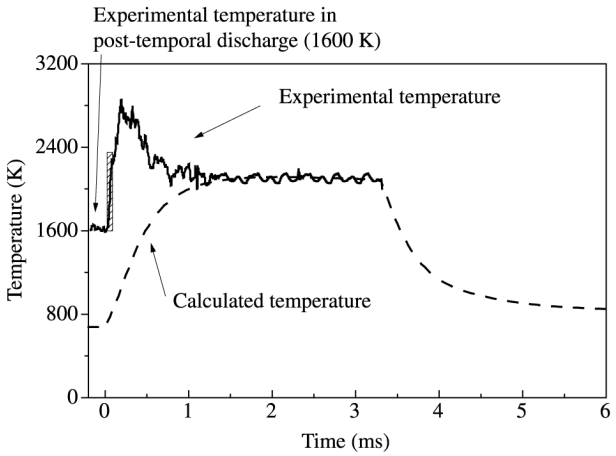

Figure 13. Time-resolved H_α temperature (gas temperature) in the surface wave configuration (915 MHz). Plasma conditions: in-pulse power 12 kW, off-pulse power 3 kW, 2000 Pa, duty cycle 10%, gas velocity 20 ms^{-1}, measurement at the gap. Comparison with the gas temperature obtained from experiments (H_α temperature) and from modeling.

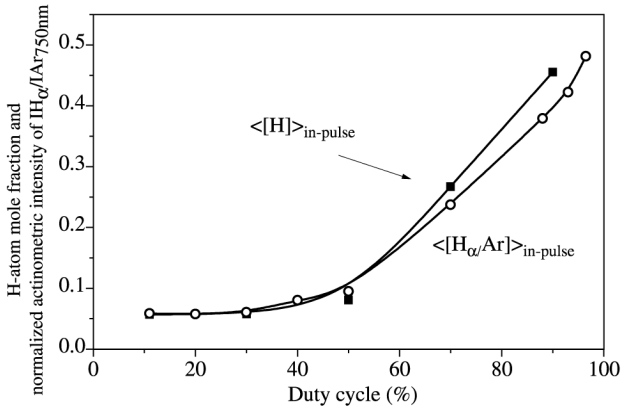

Figure 15. Variations of the H-atom mole fraction and measured actinometric ratios $I_{H\alpha}/I_{Ar}$ averaged over a period as a function of the duty cycle. In-pulse power 12 kW, off- pulse power 3kW, pulse duration 3 ms, period variation from 3.3 ms up to 30 ms.

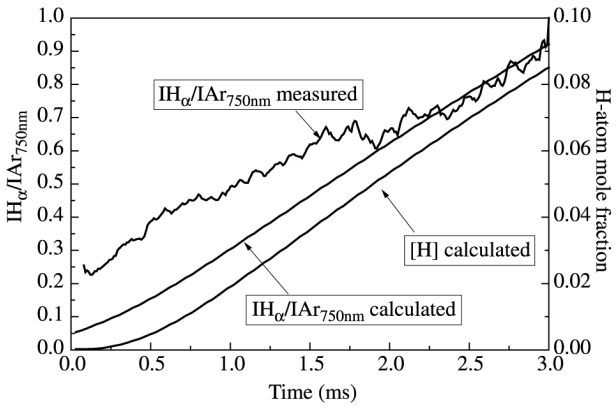

Figure 14. Time-resolved calculated and measured actinometric ratios $I_{H\alpha}/I_{Ar}$, (the calculated H-atom mole fraction is also reported). Plasma conditions identical as in Fig. 13.

The calculated and measured actinometric ratios $I_{H\alpha}/I_{Ar}$ are compared in Fig. 14, while the calculated H-atom mole fraction and calculated $< I_{H\alpha}/I_{Ar} >$ are reported in Fig. 15. The H-atom mole fraction reaches a value of 0.1 at the end of the pulse which is much higher than the corresponding value obtained in the MW cavity plasma (x_H = 0,01) although the gas temperature was seen to be identical. Since the weights of the thermal dissociation in the production rate of H-atom is similar for the two configurations in the considered discharge conditions, we can say that molecular hydrogen dissociation proceeds mainly through electronic process (Te = 17000 K and ne = 10^{12} cm^{-3} *vs.*15000 K and 2.10^{11} cm^{-3} respectively in the cavity configuration) in the surface wave configuration. The CH_3-radical density shows a maximum value at the mid-pulse as already observed for the cavity case.

4.3.1 Effect of duty cycle on the plasma composition and temperatures

To pursue our investigation on the interest of pulsing discharges for growing diamond, several simulations have been performed. In order to evaluate another parameter than the in-pulse power, instead of changing the in-pulse power as we did for the cavity case, here we kept it constant and varied instead the duty cycle. The interest was to observe the effect of recombination processes on the H-atom density in particular. The conditions are given in Table 1. All the simulations were performed for a pulse duration of 3 ms, an in-pulse power of 12 kW, a pressure of 2000 Pa and a H_2/5% CH_4 mixture.

Table 2 shows that as the duty cycle increases the electron temperature as well as the gas temperature decrease while the electron density is slightly increasing. Simultaneously the H-atom mole fraction strongly increases and the CH_3-radical mole fraction decreases (Fig. 16). Since the production term is controlled by the in-pulse power density, which is maintained constant, the increase in H-atom mole fraction as a function of the duty cycle can only be attributed to the decrease of the off-plasma time as the duty cycle increases, which prevents recombination of H-atom during this stage. As far as CH_3-radical density is concerned, its

Table 1. Average power as a function of the duty cycle. Surface-wave configuration with constant in-pulse power (12 kW), off-pulse power (3 kW), pressure (2000 Pa) and plasma duration (3 ms). Excitation frequency of 915 MHz.

Period (ms)	Cyclic ratio (%)	Average power
3.33	90 %	10.8
4.2	70 %	8.4
6	50 %	6
10	30 %	3.6
30	11 %	1.3

Table 2. plasma parameters as a function of the duty cycle. Surface-wave configuration with constant in-pulse power (12 kW), off-pulse power (3 kW), pressure (2000 Pa) and plasma duration (3 ms). Excitation frequency of 915 MHz.

Duty cycle (%)	11	30	70	90
Tg	2150	2100	1950	1825
Te (K)	19000	18000	17000	16000
Xe (10^{-5})	1.3	1.3	1.4	1.4

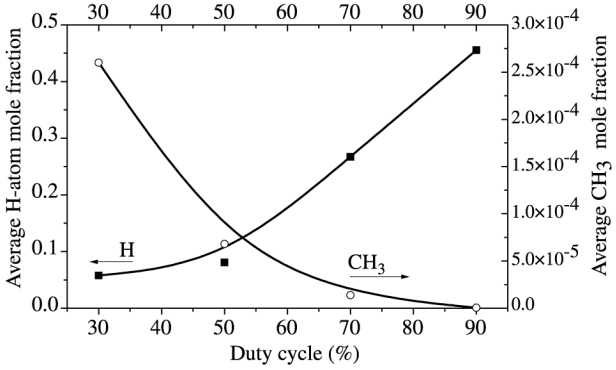

Figure 16. Variations of the H-atom mole fraction and the CH_3-radical mole fraction averaged over a period as a function of the duty cycle. Plasma conditions 915 MHz/surface wave configuration/ In-pulse power 12 kW, off- pulse power 3 kW, pulse duration 3 ms, period variation from 3.3 ms up to 30 ms.

decrease as the duty cycle increases can be easily related to the decrease in the gas temperature. As a matter of fact, Tg decreases from 2200 K to 1800 K, which corresponds exactly to the domain of sensitivity for the production of CH_3.

5. Conclusion

This paper was dedicated to the determination of new driving parameters which control the production and loss of the main active species for diamond growth (H atoms and CH_3 radicals) in pulsed plasmas relatively to continuous plasmas.

In continuous mode, the H-atom density at the diamond surface was seen to be mainly controlled by its production term in the plasma bulk and governed by the gas temperature (directly related to the microwave power density), and by the diffusion process at the plasma/diamond surface interface. The CH_3-radical density was seen to be completely controlled by the gas temperature and H-atom gradients at the plasma/diamond surface interface.

Due to the major role of power density on H-atom production, very high power must be injected to improve diamond deposition reactors. However, high thermal transfers to reactor walls lead to their strong heating. This effect was seen to be prevented by using pulsed discharges. H-atom production can be insured by very high in-pulse power density and optimal off-pulse duration, long enough to prevent wall heating and atom catalytic recombination enhancement (These are related to the time-averaged power and not to the in-pulse power density), and short enough to limit the duration of H-atom consumption phase.

In pulsed mode, additional parameters which control H-atom and CH_3-radical production and loss terms have been identified: in-pulse power density controls gas temperature and then thermal dissociation, while off-plasma time controls volumetric recombination process and H-atom consumption kinetic. Optimization of H-atom density in pulsed mode implies then a compromise between short duty cycle that allows to increase the in-pulse power keeping constant the averaged power, and short off-plasma time that limits H-atom recombination. As far as CH_3 radical is concerned, its production remains directly related to the gas temperature (in the range 1800 K to 2000 K) and H-atom density.

While in cavity configuration operating at pressure higher than 2500 Pa and power greater than 1 kW, the H-atom density was seen to be, in pulsed mode, still controlled by thermal dissociation (the in-pulse power density was always greater than 12 Wcm^{-3}), in surface wave configuration, electronic dissociation was seen to play an important role. As a matter of fact, with this configuration, pressure of around 2000 Pa was currently used, and in addition the excitation frequency was lower than in the cavity configuration (915 MHz instead of 2.45 GHz). The way as the power is coupled to the plasma leads to much larger plasma volume than in the cavity configuration, leading to lower power density for identical injected power. Furthermore, according to the gas velocity, which can be varied

from 1 to 60 ms^{-1}, the gas temperature can be lowered substantially even while a high in-pulse power is injected. For this configuration, gas velocity and electron temperature and density became therefore new determining parameters for optimizing the reactor in the aim of depositing diamond films.

Acknowledgements

This work has received a financial support from DGA.

References

1. Harris, S.J. *Appl. Phys. Lett.*, v. 56, n. 23, p. 2298, 1990.
2. Goodwin, D.G. *J. Appl. Phys.*, v. 74, n. 11, p. 6888, 1993.
3. Butler, J.E.; Woodin, R.L. *Phil. Trans. R. Soc. Lond. A*, v. 342, p. 209, 1993.
4. Gicquel, A.; Silva, F.; Hassouni, K. *J. Electrochem. Soc.*, v. 147, n. 6, p. 2218, 2000.
5. Hassouni, K.; Leroy, O.; Farhat, S.; Gicquel, A. *Plasma Chem. Plasma Process.*, v. 18, p. 325, 1998.
6. Lombardi, G.; Duten, X.; Hassouni, K.; Gicquel, A.; Rousseau, A. submitted to *J. Electrochem. Soc.*, 2002.
7. Cappelli, M.A.; Owano, T.G.; Gicquel, A.; Duten, X. *Plasma Chem. Plasma Process.*, v. 20, n. 1, p. 1-12, 2000.
8. Hassouni, K.; Duten, X.; Rousseau, A.; Gicquel, A. *Plasma Sources Sci. Technol.*, v. 10, p. 61, 2001.
9. Gicquel, A.; Chenevier, M.; Hassouni, K.; Tserepi, A.; Dubus, M. *J. Appl. Phys.*, v. 83, n. 12, p. 7504, 1998.
10. Duten, X.; Rousseau, A.; Gicquel, A.; Leprince, P. *J. Appl. Phys.*, v. 86, n. 9, p. 5299, 1999.
11. Duten, X.; Rousseau, A.; Hassouni, K.; Leprince, P.; Gicquel, A. submitted to *J. Phys. D.*, 2002.
12. Zalicki, P.; Ma, Y.; Zare, R.N.; Wahl, E.H.; Owano, T.G.; Kruger, C.H. *Appl. Phys. Lett.*, v. 67, n. 1, p. 144, 1995.
13. Childs, M.A.; Menningen, K.L.; Chevako, P.; Spellmeyer, N.W.; Anderson, L.W.; Lawler, J.E. *Phys. Lett.* A, v. 171, p. 87, 1992.
14. Loh, M.H.; Cappelli, M.A. *Appl. Phys. Lett.*, v. 70, n. 8, p. 1052, 1997.
15. Hassouni, K.; Grotjohn, T.A.; Gicquel, A. *J. Appl. Phys.*, v. 86, p. 134, 1999.
16. Capitelli, M.; Colonna, G.; Hassouni, K.; Gicquel, A.; *Plasma Chem. Plasma Process.*, v. 16, n. 2, p. 153, 1996.
17. Hassouni, K.; Gicquel, A.; Capitelli, M.; Loureiro, J.; *Plasma Sources Sci. Technol.*, v. 8, n. 3, p. 494, 1999.
18. Krasnoperov, L.N.; Kalinovski, I.J.; Chu, H.N.; Gutman, D.J. *J. Phys. Chem.*, v. 97, p. 11787, 1993.
19. Yos, J.M. Technical Memorandum RAD, TM-63-7, AVCO-RAD, 1963, Wilmington, Mass.
20. Gicquel, A.; Hassouni, K.; Breton, Y.; Chenevier, M.; Cubertafon, J.C. *Diamond and Related Materials*, v. 5, p. 336, 1996.
21. Gicquel, A.; Hassouni, K.; Silva, F.; Achard, J. *Current Appl. Phys.*, v. 1, p. 479, 2001.